DOI: 10.15825/1995-1191-2025-2-100-111

DEVELOPMENT AND EVALUATION OF BIODEGRADABLE SILK FIBROIN SCAFFOLDS

E.I. Podbolotova[1, 2], L.A. Kirsanova[1], E.G. Kuznetsova[1], N.V. Grudinin[1], A.R. Pashutin[1, 2], O.I. Agapova[1], A.E. Efimov[1], E.A. Nemets[1], Yu.B. Basok[1], I.I. Agapov[1]

[1] Shumakov National Medical Research Center of Transplantology and Artificial Organs, Moscow, Russian Federation

[2] Moscow Institute of Physics and Technology (National Research University), Dolgoprudny, Moscow Oblast, Russian Federation

Objective: to investigate the biodegradation of natural silk-based tissue scaffolds (NS-TS) under *in vitro* and *in vivo* conditions, assessing their potential for tissue engineering applications. **Materials and methods.** Two types of NS-TS, Fibroplen-Atlas and Fibroplen-Gas, along with their modified versions, were analyzed. *In vitro* biodegradation was assessed in Fenton's solution, while *in vivo* studies were conducted on rats, with histological and morphometric analysis of the implants at 4, 14, and 56 days post-implantation. **Results.** *In vitro* biodegradation studies showed that Fibroplen-Gas completely degraded in <15 days, whereas Fibroplen-Atlas persisted for up to 45 days. *In vivo* analysis showed gradual resorption of all scaffolds, with Fibroplen-Gas exhibiting more pronounced degradation. Histological examination revealed a macrophage response, formation of foreign-body giant cells, and signs of implant vascularization. Morphometry confirmed a reduction in filament cross-sectional area, particularly in modified samples. **Conclusion.** Modifications of NS-TS influence their biodegradation rate, inflammatory response, and vascularization.

Keywords: silk, biodegradation, tissue engineering.

INTRODUCTION

The development of biodegradable materials for wound treatment and tissue defect replacement is a key challenge in modern medicine and bioengineering. Traditional methods, such as using autologous grafts, present several limitations, including limited availability of donor material, risk of complications at donor site, potential graft rejection, and inability to fully restore the complex anatomy of damaged tissues [1, 2]. Effective tissue repair requires not only innovative techniques but also creation of new biomaterials that meet the specific requirements of clinical applications. Over recent decades, biomaterials, particularly those of natural origin, have garnered increasing attention due to their unique properties, such as biocompatibility, biodegradability, and the potential for modification to suit individual patient needs [3]. Among these biomaterials, silk has received special attention because of its outstanding physicochemical and biological properties, making it a promising foundation for the manufacture of medical devices [4].

Silk, obtained from the cocoons of Bombyx mori silkworms, is a natural protein polymer primarily composed of two key proteins: fibroin and sericin. Fibroin, in particular, possesses unique mechanical properties, such as high tensile strength and elasticity, making it highly attractive for medical applications [5, 6]. Silk is also noted for its high biocompatibility, which helps minimize the body's immune response, and its controlled biodegradability, a crucial factor for development of implantable materials designed for long-term use [7]. These properties make silk an ideal candidate for creating materials for tissue engineering and wound care [8].

In recent years, silk has been extensively researched as a foundation for the development of various medical devices. Notably, biodegradable materials based on silk fibroin have been developed for bone replacement [9, 10]. These materials, which incorporate silk fibroin, calcium phosphates, and other bioactive components, have shown promising biological performance and potential for use in bone engineering, particularly in bone defect repair. Silk is also being explored for the creation of scaffolds – three-dimensional structures that support cell growth and differentiation. Such scaffolds can be used to regenerate various tissues, including bone, cartilage, skin, nerve tissue [11–13], and even corneal tissue [14]. This approach represents a promising alternative to traditional tissue repair methods.

One of the key advantages of silk is its high flexibility in modifying its properties according to the specific requirements of a given application. By adjusting the processing conditions, it is possible to regulate the material's biodegradation rate, mechanical properties,

Corresponding author: Igor Agapov. Address: 1, Shchukinskaya str., Moscow, 123182, Russian Federation. Phone: (495) 231-60-42. E-mail: igor_agapov@mail.ru

and cell interaction, which opens up significant potential for creating personalized medical devices that can be tailored to the unique needs of individual patients [15, 16]. In addition, silk has low immunogenicity, reducing the risk of implant rejection and inflammation. This property is particularly crucial for the development of materials intended for long-term implantation [17, 18]. This makes silk especially valuable in the creation of products for treating chronic diseases and repairing damaged tissues.

Despite the clear advantages of silk, its use in medicine comes with several challenges. The production and processing of silk must be carefully controlled to ensure the stability of the material's properties and its safety for the patient. Even minor changes in the production process can significantly alter the mechanical, biological, and chemical properties of the material, necessitating stringent standards and additional research to confirm its effectiveness over the long term.

Thus, while silk shows considerable promise as a biomaterial, its application in medical technologies requires further investigation. The development of new methods for modifying and optimizing the properties of silk-based materials will open new opportunities for their successful integration into clinical practice and their use in various medical fields, including tissue engineering and tissue repair. This article explores the properties of tissue scaffolds made from natural silk, their potential for medical applications, and possible ways to to optimize their properties.

MATERIALS AND METHODS

Preparation of Fibroplen-Gas 0 and Fibroplen-Atlas 0 samples

For the fabrication of biodegradable fabric scaffolds, natural silk fabrics composed solely of silk fibers and free from extraneous impurities were used (EAC Declaration of Conformity, No. RU D-CN.PA09.B.91575/23, Tianjin Textile Industrial Supply And Sale Co., Ltd, China). Two types of silk fabrics with differing densities – 15 g/m^2 and 155 g/m^2 – were selected for this study. The preparation process for the fabric samples followed previously described protocols [19]. Initially, the fabrics were boiled in a sodium bicarbonate solution in a water bath for 40 minutes, followed by thorough rinsing in distilled water and a second boiling for 30 minutes. This cycle was repeated three times after which the scaffolds were air-dried at room temperature. The resulting samples were designated as "Fibroplen-Gas 0" (lower-density fabric) and "Fibroplen-Atlas 0" (higher-density fabric).

Preparation of modified Fibroplen-Gas 80 and Fibroplen-Atlas 80 samples

To obtain modified scaffold variants, the previously prepared Fibroplen-Gas 0 and Fibroplen-Atlas 0 samples were subjected to controlled degradation in a water-alcohol solution of calcium chloride, using a molar ratio of 1 : 2 : 8. Incubation was carried out at 46 °C for 352 minutes for Fibroplen-Gas 0 samples and 216 minutes for Fibroplen-Atlas 0 samples – corresponding to 80% of the total degradation time for each fabric type. Following incubation, the samples were thoroughly rinsed with distilled water and then air-dried at room temperature. The resulting samples are hereinafter designated as "Fibroplen-Gas 80" and "Fibroplen-Atlas 80", respectively.

In vitro biodegradation study

In vitro biodegradation of samples was evaluated in accordance with GOST 10993-13-2009 ("Assessment of biological effect of medical devices"). Samples were incubated in 40 mL of Fenton's reagent, composed of 100 μM $FeSO_4$ and 1 mM H_2O_2, at a temperature of 37 °C. The oxidative medium was renewed every 3 days. At the end of incubation, the samples were rinsed with 40 mL of distilled water, dried in a thermostat at 37 °C for 48 hours, and subsequently placed in a Binder VD-54 vacuum desiccator (Germany) at a residual pressure of 10–20 mmHg for 24 hours.

Biodegradation was assessed gravimetrically using a Sartorius CPA-225D analytical scale (Germany), by measuring the change in the sample mass before and after the incubation period.

In vivo biodegradation study

In vivo biodegradation experiment was carried out on male Wistar rats weighing 250–300 g, obtained from the Krolinfo laboratory animal nursery (Vysokovo, Orekhovo-Zuyevsky urban district, Russia). Prior to the experiment, the animals were acclimatized to the housing conditions for a period of 7 days. Throughout the study, the rats were kept isolated in single cages, they were provided with standard laboratory feed and had ad libitum access to water. Vivarium temperature was maintained at 22 ± 2 °C, relative humidity at 55–65%, and a 12-hour light/dark cycle.

Before surgery, general anesthesia was induced using Zoletil® 100 (Virbac, France) at a dose of 15 mg/kg body weight administered intramuscularly. For antiseptic preparation, a 0.05% chlorhexidine solution was applied to the skin in the interscapular region. To prevent mechanical irritation and minimize the risk of postoperative infection, the surgical site was shaved using electric clippers prior to intervention.

Following skin antisepsis, a subcutaneous pocket was created using sterile surgical scissors and a scalpel. A 1×1 cm silk scaffold sample was inserted into the prepared cavity and secured in place with four knotted sutures using Prolene 4/0 monofilament polypropylene surgical thread (Ethicon, USA). The sutures ensured close adherence of the implant to the surrounding subcutaneous tissue, thereby preventing displacement. After

implantation, the incision was closed using additional knotted sutures.

The experimental durations were set at 4, 14, and 56 days. Upon completion of each time point, the animals were euthanized. Following confirmation of biological death, the implanted materials along with surrounding tissue were explanted for subsequent histological examination.

Histological study

After explantation, tissue samples were fixed in 10% buffered formalin solution for at least 24 hours. Standard histological processing was performed, including dehydration through a graded ethanol series (50%, 60%, 70%, 80%, and 96%), paraffin embedding, and sectioning at a thickness of 5–6 μm using a RM2245 microtome (Leica, Germany).

Histological staining was performed using the following methods:

– Mayer's hematoxylin and eosin (BioVitrum, Russia) – to evaluate the overall tissue structure;
– Masson's trichrome stain (BioVitrum, Russia) – to detect total collagen.

The preparations were examined using an Eclipse 50i optical microscope (Nikon, Japan) equipped with a digital camera.

The histological evaluation focused on the following parameters:

– Cellular response (presence of macrophages, foreign-body giant cells, lymphocytes, and granulocytes);
– Vascularization (capillary formation);
– Formation of connective tissue capsules;
– Degree of material bioresorption.

Morphometric analysis

Morphometric evaluation of the filament cross-sectional area was conducted using ImageJ software (version 1.49v, National Institutes of Health, USA). For each filament type, 40 cross-sections with clearly defined contours and free from overlapping neighboring structures were selected for analysis.

Statistical data processing

Statistical analysis was performed using IBM SPSS Statistics version 26. Data distribution was assessed using the Kolmogorov–Smirnov test. The following statistical tests were applied:

– Mann–Whitney U test – for comparison between two independent groups;
– Kruskal–Wallis test – for comparison among three or more independent groups;
– Tukey's test – for post hoc multiple comparisons.

Differences were considered statistically significant at $p < 0.05$. For variables with non-normal distribution, data are presented as median (Me) and interquartile range (Q1–Q3).

RESULTS AND DISCUSSION

In vitro biodegradation studies

The Fibroplen-Atlas silk samples with different pretreatments showed varying rates of biodegradation (Table 1). For Fibroplen-Atlas 0 samples, slow degradation was observed on day 15, with a weight loss of 5%. By day 30, degradation accelerated, reaching a mass loss of 44%, and by day 45, the total weight loss amounted to 79%. In contrast, Fibroplen-Gas samples underwent complete degradation in less than 15 days. For each time point, five samples of each type were analyzed.

Table 1

Effect of pretreatment on silk degradation profile

	15 days	30 days / Δ 15–30 days	45 days / Δ 30–45 days
Fibroplen-Atlas 0	5%	44% / 39%	79% / 35%
Fibroplen-Atlas 80	5%	49% / 44%	86% / 37%
Fibroplen-Gas	All samples were completely degraded in less than 15 days		

The results obtained indicate that pretreatment of silk has an effect on its biodegradation *in vitro* biodegradation rate. Therefore, the choice of material treatment may play a critical role in developing materials with the required degradation rate for various biomedical applications.

In vivo biodegradation studies (morphologic analysis)

Implantation at day 4 (unmodified samples)

Fibroplen-Gas 0

On day 4 following implantation of the control Fibroplen-Gas 0 sample, histological examination revealed a large fragment of transverse striated muscle tissue, surrounded by a thin fibrous layer and loose connective tissue (Fig. 1, a). Within this area, implant fragments were identified as homogeneous filaments observed in both transverse and longitudinal sections. These filaments showed a delicate cream coloration with hematoxylin and eosin staining and appeared pale pink with Masson's trichrome stain.

A moderate cellular response to the implant was observed, characterized by the presence of macrophages, foreign-body giant cells (FBGCs), a few lymphocytes, and occasional granulocytes. Only faint signs of macrophage-mediated resorption of the implant material was noted. No signs of inflammation were detected in the surrounding muscle tissue. Overall, inflammatory response was mild and primarily lymphoid-macrophage in nature.

Fibroplen-Atlas 0

Fig. 1, b presents the histological image of the control sample "Fibroplen-Atlas 0", demonstrating a fragment

of transverse striated muscle tissue adjacent to a fibrous layer and loose connective tissue, within which the implant was identified. Surrounding the implant, there is loose connective tissue with pronounced hypercellularity, characterized by a high concentration of fibroblasts, histiocytes, and lymphocytes, as well as numerous full-blooded capillaries. This morphological pattern is indicative of active granulation tissue formation.

The content of FBGCs was very low, with only occasional individual cells detected. While granulocytes were generally scarce in the surrounding tissue, a localized area of intense cellular infiltration was identified, suggesting the presence of a residual acute inflammatory response. There were virtually no signs of bioresorption.

Implantation at day 14 (unmodified samples)

Fibroplen-Gas 0

The examined sample contains adipose tissue, within which the Fibroplen-Gas 0 implant was located (Fig. 2, a). The implant fragments were surrounded by thin connective tissue strands, interspersed with thin-walled, full-blood blood vessels, indicating ongoing processes of encapsulation and vascularization. Numerous macrophages and FBGCs were observed in close proximity to the implant strands, along with clear signs of bioresorption. In addition, few lymphocytes and occasional granulocytes were detected. The inflammatory response was predominantly macrophage-mediated.

Fibroplen-Atlas 0

The implant is surrounded by loose connective tissue along its perimeter (Fig. 2, b). In close proximity to the implant, thin connective tissue strands oriented parallel to its long axis were observed, which likely indicate early stages of capsule formation. Connective tissue fibers and thin-walled blood vessels were seen infiltrating the implant. Numerous macrophages, FBGCs, and epithelioid cells were present around the implant filaments.

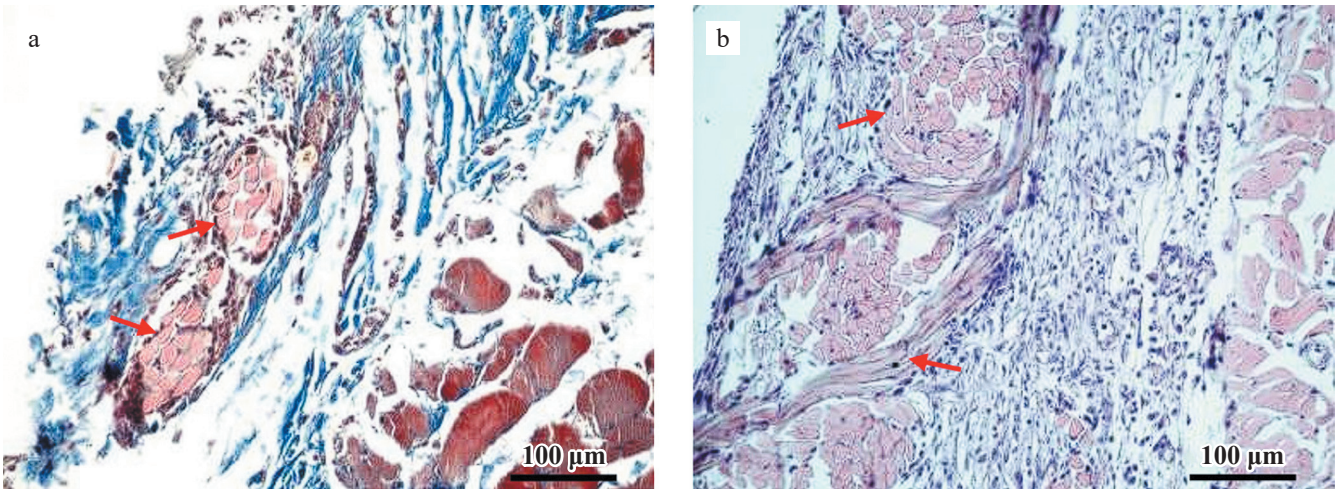

Fig. 1. Samples at 4 days post-implantation: a, Fibroplen-Gas 0, H&E stain; b, Fibroplen-Atlas 0, H&E stain. Arrows indicate implant fragments. 200×

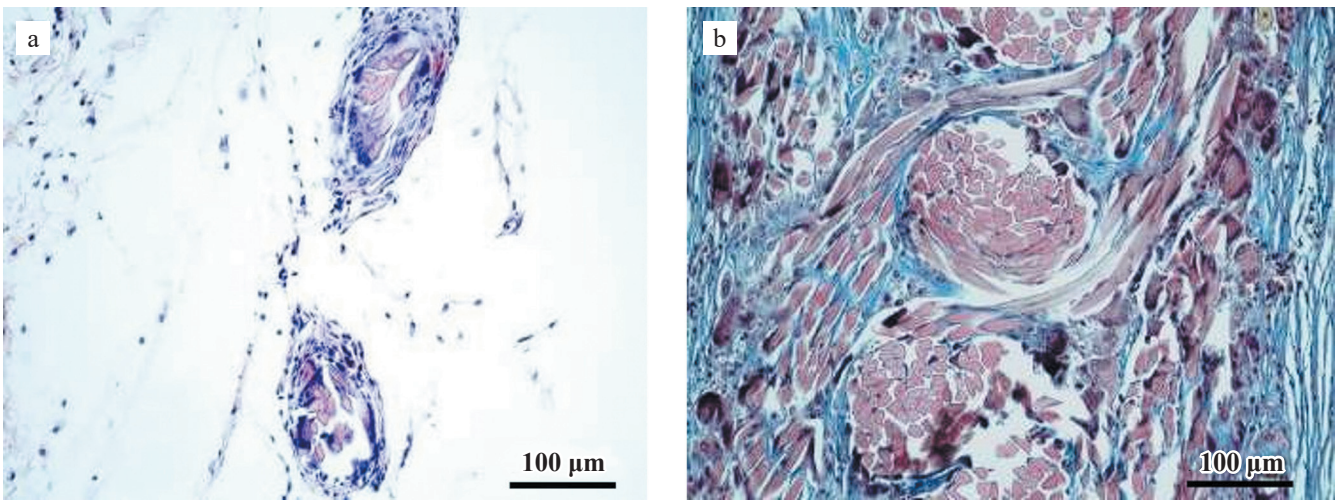

Fig. 2. Samples at 14 days post-implantation: a, Fibroplen-Gas 0, H&E stain; b, Fibroplen-Atlas 0, Masson's trichrome stain. 200×

However, signs of bioresorption were minimal, with the majority of the implant material remaining structurally intact. Overall, the inflammatory response was predominantly macrophage-mediated, with small admixture of lymphocytes and occasional granulocytes.

Implantation at day 56 (unmodified samples)

Fibroplen-Gas 0

The implant is embedded in a layer of loose connective tissue, adjacent to fragments of transverse striated muscle tissue (Fig. 3, a). A sustained macrophage response is evident, including the presence of FBGCs, accompanied by partial resorption of the implant material. Vascularization persists, with thin-walled capillaries noted in the surrounding tissue. A thin connective tissue capsule has formed along the implant perimeter, and in some areas, it is penetrated by capillaries. Besides, individual filaments of the implant are enveloped by collagen fibers. Compared to the 14-day observation period, both the signs of bioresorption and encapsulation of the implant threads appear more pronounced.

Fibroplen-Atlas 0

The implant is surrounded by loose connective and adipose tissue (Fig. 3, b). The inflammatory response remains mild and predominantly macrophage-mediated. FBGCs are scarce and primarily located in the peripheral zone of the implant adjacent to surrounding tissues. A substantial portion of the implant material appears structurally intact, showing minimal signs of resorption. Vascularization is evident, with full-blooded capillaries observed among the implant filaments. A thin connective tissue capsule has formed around the implant, with occasional capillary penetration. Besides, individual strands of the implant are encapsulated by collagen fibers.

Implantation at day 4 (modified samples)

Fibroplen-Gas 80

The histological profile is characterized by transverse striated muscle tissue adjacent to a broad layer of loose connective tissue exhibiting signs of inflammatory infiltration (Fig. 4, a). The infiltrate includes granulocytes, lymphocytes, mast cells, macrophages, numerous full-blooded capillaries, and fibroblasts – indicative of active granulation tissue formation. Single FBGCs are locally present. Notably, in comparison to the unmodified Fibroplen-Gas 0 samples at the same time point, inflammatory response in the modified samples is more pronounced and polymorphic, whereas the unmodified implants evoked a milder, predominantly lymphoid-macrophage reaction.

Fibroplen-Atlas 80

In the examined sample, the histological profile consists of transverse striated muscle tissue bordered by a thin fibrous layer and a layer of loose connective tissue. Along the boundary, numerous implant fragments are identified, primarily as transverse and, less frequently, longitudinal sections of filaments (Fig. 4, b). Inflammatory response is characterized by abundant macrophages, the presence of FBGCs, and lymphocytes. Granulocytes are sparse and predominantly localized within the lumens of capillaries in the loose connective tissue. Evidence of implant resorption is present, mediated by both FBGCs and individual macrophages infiltrating between implant threads. Thin-walled blood vessels containing erythrocytes are observed within the implant structure. The adjacent muscle tissue appears unaltered.

It should be noted that at the same observation period, unmodified Fibroplen-Atlas 0 samples displayed features of an incomplete acute inflammatory phase, while the

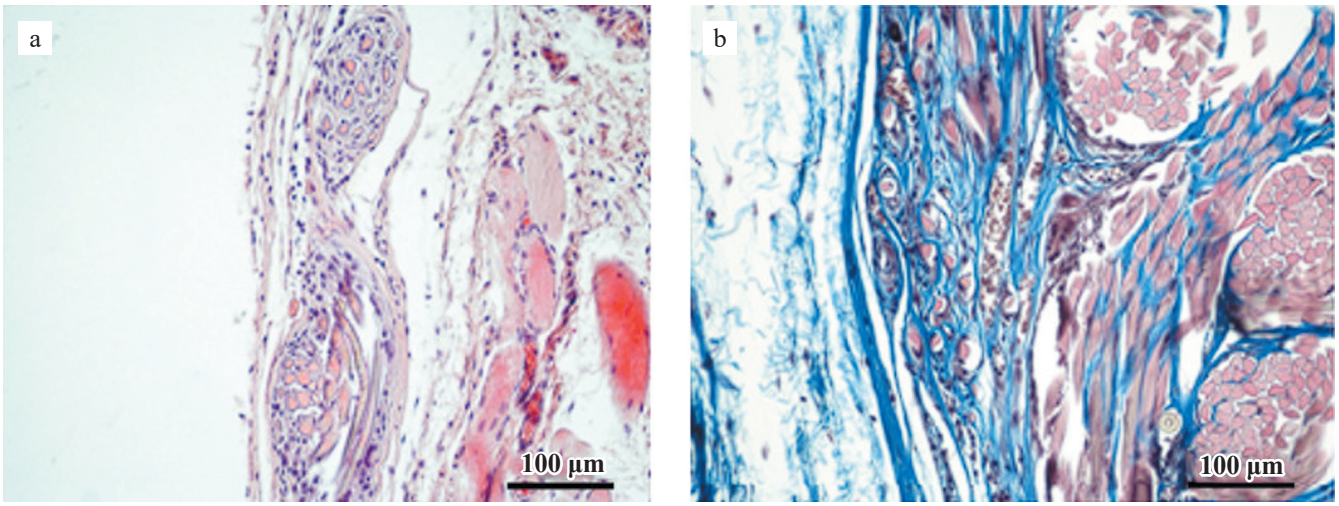

Fig. 3. Samples at 56 days post-implantation: a, Fibroplen-Gas 0, H&E stain; b, Fibroplen-Atlas 0, Masson's trichrome stain. 200×

response in Fibroplen-Atlas 80 samples shifted toward a more organized lymphoid-macrophage pattern.

The histological evaluation of the modified samples at the 4-day observation point revealed the following key features:

a) In Fibroplen-Gas 80 samples, characteristic signs of the acute phase of inflammatory response were observed, whereas the Fibroplen-Atlas 80 samples exhibited a predominantly lymphoid-macrophage type of inflammation.
b) All samples showed evidence of partial bioresorption of the implanted material. Notably, in the Fibroplen-Atlas 80 group, the implant exhibited good structural preservation, with the majority of the material remaining intact.
c) Signs of vascularization were identified only in one of the presented samples – Fibroplen-Atlas 80.
d) Fibroplen-Gas 80 samples exhibited moderate inflammation in the tissues surrounding the implant.

Implantation at day 14 (modified samples)

Fibroplen-Gas 80

In the examined specimen, the implant was surrounded by loose connective tissue (Fig. 5, a). A macrophage response to the implant was noted, accompanied by the formation of numerous FBGCs and partial resorption of the implant. The inflammatory infiltrate also contained single lymphocytes and granulocytes. Evidence of vascularization was noted within the implant, represented by the presence of isolated capillaries. Encapsulation was generally poorly developed; however, intensive ingrowth of connective tissue fibers into the implant structure was evident. The surrounding loose connective tissue showed no visible changes.

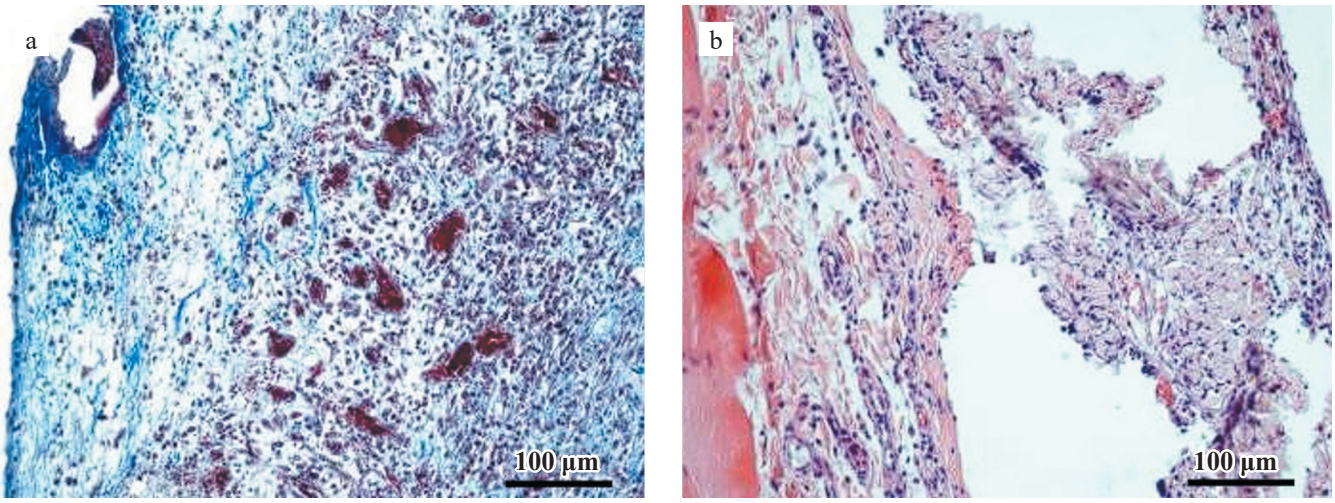

Fig. 4. Samples at 4 days post-implantation: a, Fibroplen-Gas 80, Masson's trichrome stain; b, Fibroplen-Atlas 80, H&E stain. 200×

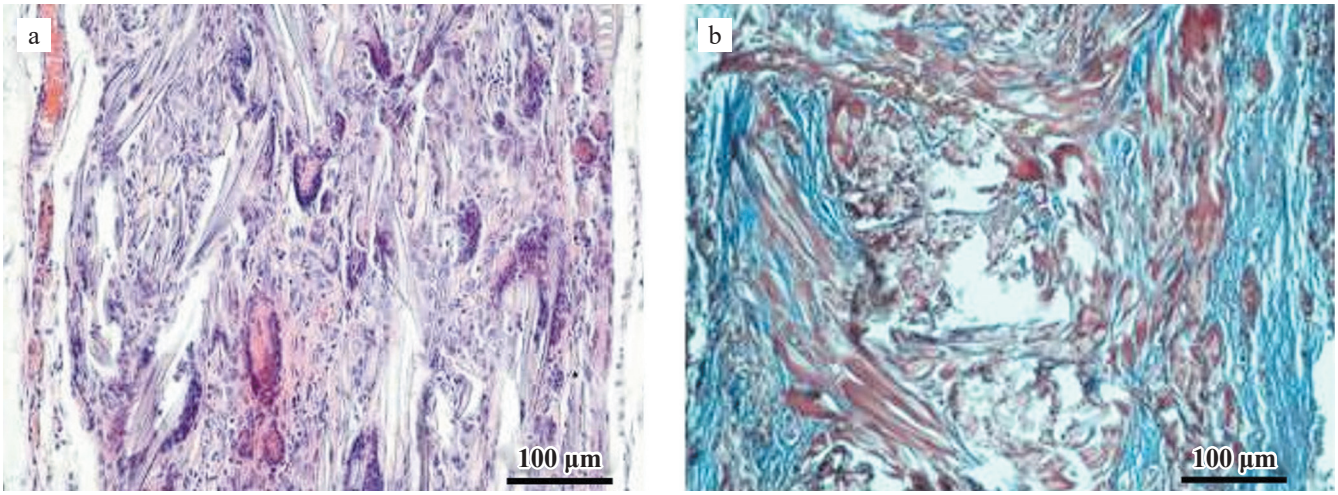

Fig. 5. Samples at 14 days post-implantation: a, Fibroplen-Gas 80, H&E stain; b, Fibroplen-Atlas 80, Masson's trichrome stain. 200×

Comparable results were observed in the unmodified Fibroplen-Gas 0 samples at the same time point. These included a predominantly macrophage-driven inflammatory response, ingrowth of connective tissue strands into the implant, as well as signs of bioresorption and vascularization.

Fibroplen-Atlas 80

The histological examination shows the implant surrounded by loose connective tissue (Fig. 5, b). A loose, unevenly thick connective tissue capsule is present around the implant's perimeter. A lymphoid-macrophage inflammatory response involving FBGCs is noted. Compared to Fibroplen-Gas 80 samples, a slightly higher number of lymphocytes is observed. Evidence of partial resorption of the implant is also present. Signs of vascularization and ingrowth of connective tissue strands into the implant are apparent. The adjacent loose connective tissue contains full-blooded capillaries, increased number of lymphocytes and macrophages (relative to previous samples), as well as isolated plasmocytes.

The overall morphologic picture is generally consistent with that observed in the experiment using unmodified Fibroplen-Atlas samples at the same time point. However, it should be noted that the degree of fibrosis, vascularization, and bioresorption is greater in the modified samples compared to their unmodified counterparts. In addition, differences were observed in the composition of the inflammatory infiltrate: specifically, a slightly higher number of lymphocytes was recorded in the modified samples, and the inflammatory response exhibited a more pronounced lymphoid-macrophage character.

The histological features observed in the modified Fibroplen-Gas 80 and Fibroplen-Atlas 80 samples at 14 days post-implantation can be summarized as follows:

a) A predominance of the gigantocellular component in the inflammatory infiltrate, most notably in the Fibroplen-Gas 80 sample.
b) Formation of a connective tissue capsule around the implant, with the least pronounced capsule observed in the Fibroplen-Gas 80 group.
c) Ingrowth of connective tissue fibers into the implant, partially replacing the original material.
d) Evidence of implant vascularization.
e) Partial resorption of implant material.

Implantation at day 56 (modified samples)

Fibroplen-Gas 80

In the examined specimen, the Fibroplen-Gas 80 implant was localized within a layer of loose connective tissue (Fig. 6, a). A macrophage-dominated inflammatory response was observed, with the presence of FBGCs and signs of ongoing resorption of the implant material. Vascularization within the implant was minimal, with only isolated capillaries identified. There was no formed connective tissue capsule encasing the implant; instead, encapsulation was limited to individual threads and/or fibers. The adjacent loose connective tissue showed no apparent changes.

It is worth noting that these findings partially resemble those seen in the control group (Fibroplen-Gas 0), particularly regarding the macrophage-driven inflammatory response and limited vascularization. However, unlike the modified samples, the control group showed the formation of a continuous encapsulating capsule around the implant, along with more pronounced signs of bioresorption.

Fibroplen-Atlas 80

The histological picture reveals the implant surrounded by loose connective tissue and a fragment of adjacent transverse striated muscle tissue (Fig. 6, b). A macrophage-dominated inflammatory response is evident, including the presence of FBGCs, accompanied by ongoing resorption of the implant material. Vascularization within the implant is minimal, with only isolated

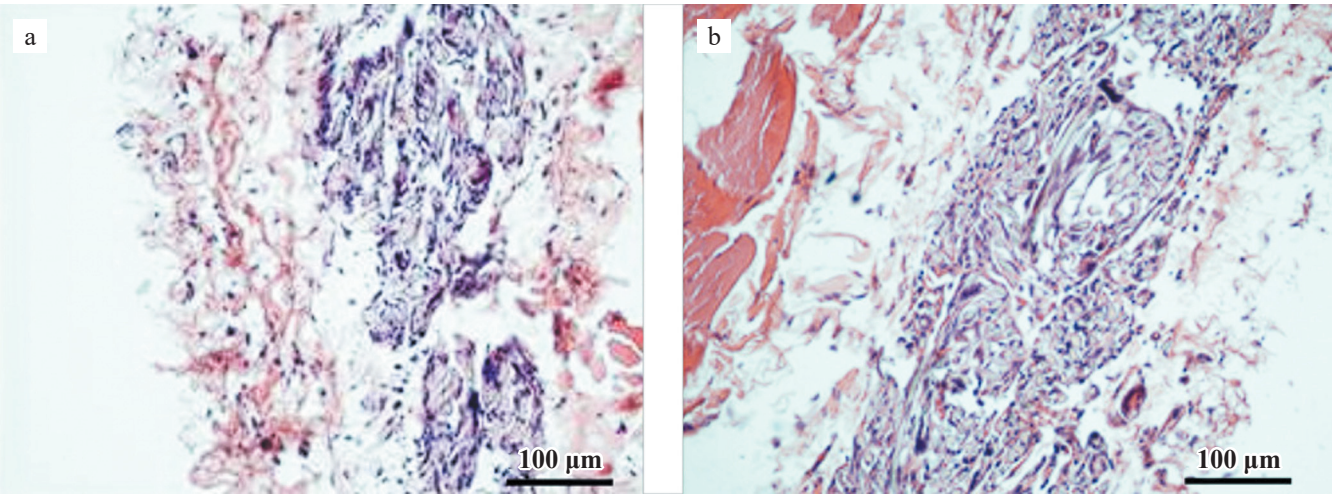

Fig. 6. Samples at 56 days post-implantation: a, Fibroplen-Gas 80, H&E stain; b, Fibroplen-Atlas 80, H&E stain. 200×

Table 2

Cross-sectional areas of Fibroplen-Gas and Fibroplen-Atlas filaments at different implantation dates

Description	Cross-sectional area, μm²			Statistical significance (p)
	4 days	14 days	56 days	
Fibroplen-Gas 0	132.5 (111.8–157.6)	86.3 (68.4–102.9)	56.7 (42.1–71.0)	$p_{4–14} < 0.05$*
				$p_{4–56} < 0.05$*
				$p_{14–56} < 0.05$*
Fibroplen-Gas 80	84.6 (60.6–102.9)	47.5 (25.5–66.8)	54.2 (41.0–71.5)	$p_{4–14} < 0.05$*
				$p_{4–56} < 0.05$*
				$p_{14–56} > 0.05$
Fibroplen-Atlas 0	121.8 (101.3–134.7)	111.3 (102.6–120.2)	97.5 (81.2–117.3)	$p_{4–14} > 0.05$
				$p_{4–56} < 0.05$*
				$p_{14–56} > 0.05$
Fibroplen-Atlas 80	48.1 (40.8–62.0)	44.4 (31.5–52.8)	31.6 (22.7–41.7)	$p_{4–14} > 0.05$
				$p_{4–56} > 0.05$*
				$p_{14–56} > 0.05$*

* sample differences are statistically significant at $p < 0.05$.

capillaries observed. No continuous connective tissue capsule around the implant; however, encapsulation of individual implant strands by collagen fibers is noted. No pathological alterations were identified in the tissue adjacent to the implant.

In the control samples (Fibroplen-Atlas 0) examined at the same time point, a similar macrophage response was observed, though it appeared less intense. Moreover, a greater portion of the implant material remained intact, showing no signs of bioresorption. Besides, a thin but continuous connective tissue capsule was observed around the implant in the control group.

The morphological study of Fibroplen-Gas and Fibroplen-Atlas samples with varying degrees of modification at 56 days post-implantation revealed the following:

a) A macrophage response to the implant, involving FBGCs and partial resorption of the material, persisted. However, compared to the previous observation period, the intensity of the cellular response was notably reduced.
b) Vascularization within the implant was minimal across all samples, though it was more pronounced in the Fibroplen-Atlas 80 group compared to Fibroplen-Gas 80.
c) No organized, restrictive fibrous capsule was observed around the perimeter of the implant.

Morphometric analysis of filament cross-sectional area

To assess the biodegradation of silk filaments in Fibroplen-Gas and Fibroplen-Atlas samples with varying levels of modification, the cross-sectional areas of the filaments were measured. The results are presented as medians and interquartile ranges (Q1–Q3) in Table 2.

The data obtained indicate that for the control Fibroplen-Gas 0 samples, the median values of filament cross-sectional areas significantly decreased ($p < 0.05$) throughout the study period. For Fibroplen-Gas 80 filaments, a significant reduction in the filament cross-sectional area occurred between 4 and 14 days of implantation. However, from 14 to 56 days of implantation, there was no significant change in the size of the filaments.

The table also reveals that in both Fibroplen-Atlas 0 and Fibroplen-Atlas 80 samples, there was a significant decrease in filament cross-sectional area between 4 and 56 days of implantation.

CONCLUSION

The conducted studies showed varying degrees of biodegradation of the Fibroplen-Gas and Fibroplen-Atlas silk materials in both *in vitro* and *in vivo* experiments.

In the *in vitro* studies, it was observed that Fibroplen-Gas silk samples underwent complete degradation in less than 15 days. In contrast, all Fibroplen-Atlas samples exhibited slow degradation in the early stages of the experiment. However, by 30 days of incubation in Fenton's solution, the rate of mass loss accelerated significantly, continuing at an increased pace until 45 days. The total mass loss reached 76–86%. Based on experimental data, it can be concluded that the choice of pretreatment method significantly influences the degradation rate *in vitro*, with Fibroplen-Gas samples showing a notably faster degradation compared to the Fibroplen-Atlas 0 samples.

As a result of the conducted morphological study, it was found that for the control Fibroplen-Gas 0 samples (implantation period of 4 days), the degree of inflammatory reaction was less pronounced and exhibited a lymphoid-macrophage character. This was in contrast to the modified samples, where signs of the acute phase of the inflammatory reaction were observed at the same experimental time point.

In the control Fibroplen-Atlas 0 samples, some signs of incomplete acute phase of the inflammatory process persisted. However, in the modified Fibroplen-Atlas 80

samples, inflammatory response was characterized as lymphoid-macrophagic at this stage.

In the control samples (Fibroplen-Atlas 0), bioresorption signs were weakly expressed and not clearly visible. In contrast, in the modified samples, particularly Fibroplen-Atlas 80, the first signs of bioresorption and vascularization were already evident at this observation period. At the 14-day observation period, the morphological study of all Fibroplen-Gas samples yielded similar results: inflammatory reaction was primarily macrophage-driven, with connective tissue strands detected within the implant. Signs of partial bioresorption and vascularization of the implant were also noted.

In contrast, at the same observation period for all Fibroplen-Atlas samples, the morphological picture shared common features: signs of bioresorption, vascularization of the implant, and growth of connective tissue fibers both on the surface and within the implant were noted. However, the degree of vascularization and fibrosis was more pronounced in the modified samples compared to the control (unmodified) samples. Additionally, some differences were observed in the inflammatory infiltrate composition. The Fibroplen-Atlas 80 samples showed a slightly higher lymphocyte content, and the reaction had a lymphoid-macrophage character. In comparison, the Fibroplen-Atlas 0 samples displayed a macrophage-driven inflammatory response.

At the 56-day observation period, histological examination of both unmodified and modified samples revealed the following features: in all samples, there was a continuation of the macrophage reaction to the implant, with the involvement of FBGCs and partial bioresorption of the material. The largest proportion of intact material was preserved in the Fibroplen-Atlas 0 sample. Compared to the 14-day period, the degree of cellular reaction was significantly reduced, most notably in the Fibroplen-Atlas 0 sample.

Vascularization was minimal across all samples, though it was more noticeable in the Fibroplen-Atlas samples. An organized restrictive connective tissue capsule around the perimeter of the implant was observed only in the Fibroplen-Atlas 0 and Fibroplen-Gas 0 samples. In all the samples, there were episodes of encapsulation of individual threads of the implant material by collagen fibers.

In the morphometric analysis of the histological samples, conducted using the ImageJ program, it was found that the cross-sectional areas of the Fibroplen-Gas 0 filaments significantly decreased throughout the study. For the Fibroplen-Gas 80 filaments, a significant decrease in cross-sectional area occurred from day 4 to day 14 of implantation. In the Fibroplen-Atlas 0 and Fibroplen-Atlas 80 samples, the filament areas significantly decreased from day 4 to day 56 of implantation. In the Fibroplen-Atlas 80 samples, a significant decrease in the cross-sectional area of the filaments was also noted from day 14 to day 56 of implantation.

FINDINGS

The following conclusions can be drawn based on the results of the conducted research:

1. Pretreatment influences the degradation rate *in vitro*. The degradation rate for modified Fibroplen-Atlas samples was higher compared to the unmodified samples. Notably, Fibroplen-Gas samples were completely degraded in less than 15 days.
2. Results of morphological study:
   a) Fibroplen-Atlas 0 samples had the largest proportion of intact material after 56 days.
   b) Signs of incomplete acute-phase inflammation were observed at the 4-day period in the Fibroplen-Gas 80 and Fibroplen-Atlas 0 samples. From the 14-day observation onward, inflammatory response in the Fibroplen-Atlas 80 sample was lymphoid-macrophage in character, while the Fibroplen-Gas and Fibroplen-Atlas 0 samples exhibited a macrophage-type reaction. By the 56-day observation period, all studied samples exhibited a macrophage-driven (predominantly gigantocellular) reaction.
   c) Partial bioresorption was observed as early as the 4-day period in the modified Fibroplen-Gas and Fibroplen-Atlas samples, involving FBGCs and single macrophages. In contrast, bioresorption was not visible in the unmodified samples at this time. Starting from day 14, bioresorption was noted in all the studied samples.
   d) Vascularization was only observed at the 4-day period in the Fibroplen-Atlas 80 sample. In all other samples, signs of vascularization were evident from the 14-day observation period onward.
   e) Signs of formation of a restrictive capsule along the perimeter of the implant were seen by the 14-day period in most of the samples. However, by day 56, a thin connective tissue capsule was observed only in the control samples Fibroplen-Atlas 0 and Fibroplen-Gas 0. All samples, regardless of modification, exhibited signs of fibrosis, including the growth of connective tissue fibers deep into the implant and episodes of encapsulation of individual implant threads by collagen fibers.
3. Morphometric analysis of histological specimens showed that the cross-sectional area of Fibroplen-Gas 0 filaments significantly decreased throughout the entire study period. For Fibroplen-Gas 80, a significant decrease was observed between days 4 and 14, with no further significant changes up to day 56. In contrast, both Fibroplen-Atlas 0 and Fibroplen-Atlas 80 samples showed a significant decrease in filament area from day 4 to day 56. Notably, in Fib-

roplen-Atlas 80, there was an additional significant reduction between days 14 and 56.

These findings confirm that modification of silk-based scaffolds enables targeted tuning of their biodegradation rate, inflammatory response, and vascularization profile. The ability to regulate these parameters provides valuable flexibility for tailoring biomaterials to specific clinical needs – such as wound healing and the development of biodegradable implants.

The authors declare no conflict of interest.

REFERENCES

1. *Dionigi B, Fauza DO*. Autologous approaches to tissue engineering. In: StemBook [Internet]. Cambridge (MA): Harvard Stem Cell Institute; 2008. 2012 Dec 10. doi: 10.3824/stembook.1.90.1.
2. *Williams D.* Challenges with the development of biomaterials for sustainable tissue engineering. *Front Bioeng Biotechnol*. 2019 May 31; 7: 127. doi: 10.3389/fbioe.2019.00127.
3. *Sevastianov VI, Basok YuB, Baranova NV, Belova AD, Grigoriev AM, Kholodenko IV et al.* Biomimetics of Extracellular Matrices for Cell and Tissue Engineered Medical Products / Eds. V. Sevastianov and Yu. Basok. Cambridge Scholars Publishing; 2023.
4. *Sahoo JK, Hasturk O, Falcucci T, Kaplan DL.* Silk chemistry and biomedical material designs. *Nat Rev Chem*. 2023 May; 7 (5): 302–318. doi: 10.1038/s41570-023-00486-x.
5. *Kamalathevan P, Ooi PS, Loo YL.* Silk-based biomaterials in cutaneous wound healing: A systematic review. *Adv Skin Wound Care*. 2018 Dec; 31 (12): 565–573. doi: 10.1097/01.ASW.0000546233.35130.a9.
6. *Kundu B, Rajkhowa R, Kundu SC, Wang X.* Silk fibroin biomaterials for tissue regenerations. *Adv Drug Deliv Rev*. 2013 Apr; 65 (4): 457–470. doi: 10.1016/j.addr.2012.09.043.
7. *Cao Y, Wang B.* Biodegradation of silk biomaterials. *Int J Mol Sci*. 2009 Mar 31; 10 (4): 1514–1524. doi: 10.3390/ijms10041514. PMID: 19468322; PMCID: PMC2680630.
8. *Vidya M, Rajagopal S.* Silk fibroin: A promising tool for wound healing and skin regeneration. *Int J Polym Sci*. 2021 Oct; 2021 (6): 1–10. doi: 10.1155/2021/9069924.
9. *Sofia S, McCarthy MB, Gronowicz G, Kaplan DL.* Functionalized silk-based biomaterials for bone formation. *J Biomed Mater Res*. 2001 Jan; 54 (1): 139–148. doi: 10.1002/1097-4636(200101)54:1<139::AID-JBM17>3.0.CO;2-7.
10. *Klimentyev AA, Naboka VA.* Biological characteristics of the biodegradable material for bone repair. *Medicine: theory and practice*. 2021; 3: 6–9. [In Russ, English abstract].
11. *Kotliarova MS, Arkhipova AYu, Moysenovich AM, Kulikov DA, Molochkov AV, Moysenovich MM.* Trehmernye poristye skaffoldy na osnove fibroina shelka dlya vosstanovleniya kostnoy tkani. *Genes & Cells*. 2017; 12 (3): 131–132. [In Russ]. doi: 10.23868/gc120968.
12. *Liu Q, Huang J, Shao H, Song L, Zhang Y*. Dual-factor loaded functional silk fibroin scaffolds for peripheral nerve regeneration with the aid of neovascularization. *RSC Adv*. 2016; 6 7683–7691. doi: 10.1039/C5RA22054H.
13. *Safonova L, Bobrova M, Efimov A, Davydova L, Tenchurin T, Bogush V et al*. Silk Fibroin/Spidroin Electrospun Scaffolds for Full-Thickness Skin Wound Healing in Rats. *Pharmaceutics*. 2021 Oct 15; 13 (10): 1704. doi: 10.3390/pharmaceutics13101704.
14. *Gavrilova NA, Borzenok SA, Revishchin AV, Tishchenko OE, Ostrovkiy DS, Bobrova MM et al.* The effect of biodegradable silk fibroin-based scaffolds containing glial cell line-derived neurotrophic factor (GDNF) on the corneal regeneration process. *Int J Biol Macromol*. 2021 Aug 31; 185: 264–276. doi: 10.1016/j.ijbiomac.2021.06.040.
15. *Aigner TB, DeSimone E, Scheibel T.* Biomedical applications of recombinant silk-based materials. *Adv Mater*. 2018 May; 30 (19): e1704636. doi: 10.1002/adma.201704636.
16. *Murphy AR, Kaplan DL*. Biomedical applications of chemically-modified silk fibroin. *J Mater Chem*. 2009 Jun 23; 19 (36): 6443–6450. doi: 10.1039/b905802h.
17. *Kolesnikov AYu, Prokudina ES, Senokosova EA, Arnt AA, Antonova LV, Mironov AV et al.* Results of long-term patency and lifetime visualization of vascular patches from silk fibroin. *Clinical and Experimental Surgery. Petrovsky Journal*. 2023: 11 (3): 68–75. [In Russ, English abstract]. https://doi.org/10.33029/2308-1198-2023-11-3-68-75.
18. *Perrone GS, Leisk GG, Lo TJ, Moreau JE, Haas DS, Papenburg BJ et al.* The use of silk-based devices for fracture fixation. *Nat Commun*. 2014 Mar 4; 5: 3385. doi: 10.1038/ncomms4385. PMID: 24594992.
19. *Agapov II, Agapova OI, Efimov AE, Sokolov DYu, Bobrova MM, Safonova LA.* Sposob polucheniya biodegradiruemykh skaffoldov na osnove tkaney iz natural'nogo shelka. Patent na izobretenie RU2653428 S1, 08.05.2018.

The article was submitted to the journal on 17.02.2025